ARMY RESEARCH LABORATORY

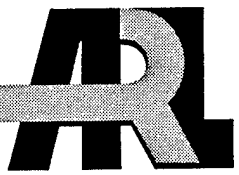

The Asymmetry Parameter and Aggregate Particles

by
Gorden Videen, Ronald G. Pinnick, Dat Ngo,
Qiang Fu, and Petr Chýlek

ARL-TR-1393 October 1997

Approved for public release; distribution unlimited.

The findings in this report are not to be construed as an official Department of the Army position unless so designated by other authorized documents.

Citation of manufacturer's or trade names does not constitute an official endorsement or approval of the use thereof.

Destroy this report when it is no longer needed. Do not return it to the originator.

Army Research Laboratory
Adelphi, MD 20783-1197

ARL-TR-1393 **October 1997**

The Asymmetry Parameter and Aggregate Particles

Gorden Videen and Ronald G. Pinnick
Information Science and Technology Directorate, ARL

Dat Ngo
Ngo Co.

Qiang Fu and Petr Chýlek
Dalhousie University

Abstract

We derive and examine the general expression for the scattering asymmetry parameter g. For aggregate particles, the asymmetry parameter is made up of two terms. One term accounts for interference effects of the electromagnetic fields radiating from the individual subsystems. The other term accounts for interaction effects of the electromagnetic fields between these subsystems. Enhanced backscatter is one phenomenon resulting from these interactions. Numerical results demonstrate that interference effects play a dominant role when the separation distance between aggregates is smaller than half the incident wavelength. As the separation distance becomes large, both interference and interaction effects drop off, and the asymmetry parameter approaches that of the individual particle constituents.

Contents

Figures

1. Introduction

The asymmetry parameter g has a long history dating back to the beginning of this century, when it was used to calculate radiation pressure exerted on particles [1]. It is currently an essential input in many radiative transfer and climate models [2]. Until recently, these models have used asymmetry parameters calculated from spherical particles, simulating water droplets and aerosol particles. Unfortunately, atmospheric particles, including ice crystals and water and aerosol particles containing contaminants, are not generally symmetric spheres. The scattering properties, including the asymmetry parameter, of these particles can vary significantly from those of spheres; e.g., both theoretical and observational work has shown that the values of the asymmetry parameter for ice crystals in cirrus clouds are significantly smaller than those given by Mie theory [3–5]. Since cirrus clouds cover about 20 to 30 percent of the earth, they influence the climate through their effects on the radiation budget [6]. A great deal of uncertainty still exists in the specification of the asymmetry parameter for cirrus clouds because of the extremely complicated shapes of ice crystals. Francis *et al.* [7] found that the deduced values of g from field experiments varied between 0.7 and 0.85. For other important radiative transfer parameters (like the extinction, scattering, and absorption efficiencies and the single scattering albedo), the anomalous diffraction approximation can provide some insight into their physical processes [8–12]. However as yet, no simple approximation can be used to calculate the asymmetry parameter.

In this report we take a closer examination of the asymmetry parameter and provide some physical insight, with the aim of stimulating further interest. We first derive the general expression for the asymmetry parameter for an arbitrary particle. Since theories have recently been developed to calculate the scatter from ensembles of particles, we consider this special case in more detail, examining specifically terms that contribute to interference and enhanced backscatter. Such theories can be used to model smoke, aerosols, and droplets containing contaminants.

2. Relevant Equations

We start by writing the general expression of the asymmetry parameter in three dimensions. We consider an arbitrarily shaped particle illuminated by a plane wave traveling in the positive z direction. For many scattering systems, such as bispheres [13–28] and spheres containing an inclusion [29–36], derivations of the scattered fields take advantage of system symmetries and the incident plane wave travels in an arbitrary direction. The appendix provides relations by which the scattering coefficients for a system illuminated by an arbitrarily incident plane wave may be converted to those for an equivalent system in which the plane wave is traveling in the positive z direction.

The scattered electric field can be expressed in terms of a vector spherical harmonic expansion as

$$\mathbf{E}^{sca} = \sum_{n=0}^{\infty} \sum_{m=-n}^{n} a_{nm}^{(j)} \mathbf{M}_{nm} + b_{nm}^{(j)} \mathbf{N}_{nm}, \tag{1}$$

where the index j on the scattering field coefficients a_{nm} and b_{nm} corresponds to what is acquired with incident plane-wave illumination polarized in the $\hat{x}$ ($j = 1$) and $\hat{y}$ ($j = 2$) directions. The vector spherical harmonics are defined by

$$\begin{aligned} \mathbf{M}_{nm} &= \hat{\theta} \left[\frac{im}{\sin\theta} h_n^{(1)}(kr) \tilde{P}_n^m(\cos\theta) e^{im\phi} \right] \\ &\quad - \hat{\phi} \left[h_n^{(1)}(kr) \frac{d}{d\theta} \tilde{P}_n^m(\cos\theta) e^{im\phi} \right], \end{aligned} \tag{2}$$

$$\begin{aligned} \mathbf{N}_{nm} &= \hat{r} \left[\frac{1}{kr} h_n^{(1)}(kr) n(n+1) \tilde{P}_n^m(\cos\theta) e^{im\phi} \right] \\ &\quad + \hat{\theta} \left[\frac{1}{kr} \frac{d}{dr} \left(r h_n^{(1)}(kr) \right) \frac{d}{d\theta} \tilde{P}_n^m(\cos\theta) e^{im\phi} \right] \\ &\quad + \hat{\phi} \left[\frac{1}{kr} \frac{d}{dr} \left(r h_n^{(1)}(kr) \right) \frac{im}{\sin\theta} \tilde{P}_n^m(\cos\theta) e^{im\phi} \right], \end{aligned} \tag{3}$$

and the wavelength of the incident plane wave is $\lambda = 2\pi/k$, $h_n^{(1)}(kr)$ are the spherical Hankel functions of the first kind, and a time dependence of $\exp(-i\omega t)$ is implicit. The normalized associated Legendre polynomials are given by

$$\tilde{P}_n^m(\cos\theta) = \sqrt{\frac{(2n+1)\,(n-m)!}{2\,(n+m)!}} P_n^m(\cos\theta). \tag{4}$$

The scattering amplitudes in the far field can be expressed by the matrix

$$\begin{pmatrix} E_\theta^{sca} \\ E_\phi^{sca} \end{pmatrix} = \frac{e^{ikr}}{-ikr} \begin{pmatrix} S_1 & S_4 \\ S_3 & S_2 \end{pmatrix} \begin{pmatrix} E_{TE}^{inc} \\ E_{TM}^{inc} \end{pmatrix}, \tag{5}$$

where E_{TM}^{inc} and E_{TE}^{inc} correspond to transverse electric and transverse magnetic incident plane wave illumination, respectively; and E_θ^{sca} and E_ϕ^{sca} correspond to scattered electric fields polarized in the $\hat{\theta}$ and $\hat{\phi}$ directions. In general, the elements of the scattering amplitude matrix can be written as

$$S_1 = \sum_{n=0}^{\infty} \sum_{m=-n}^{n} (-i)^n e^{im\phi} \times \left[b_{nm}^{(2)} \tilde{\pi}_n^m + a_{nm}^{(2)} \tilde{\tau}_n^m \right], \tag{6}$$

$$S_2 = -i \sum_{n=0}^{\infty} \sum_{m=-n}^{n} (-i)^n e^{im\phi} \times \left[a_{nm}^{(1)} \tilde{\pi}_n^m + b_{nm}^{(1)} \tilde{\tau}_n^m \right], \tag{7}$$

$$S_3 = -i \sum_{n=0}^{\infty} \sum_{m=-n}^{n} (-i)^n e^{im\phi} \times \left[a_{nm}^{(2)} \tilde{\pi}_n^m + b_{nm}^{(2)} \tilde{\tau}_n^m \right], \text{ and} \tag{8}$$

$$S_4 = \sum_{n=0}^{\infty} \sum_{m=-n}^{n} (-i)^n e^{im\phi} \times \left[b_{nm}^{(1)} \tilde{\pi}_n^m + a_{nm}^{(1)} \tilde{\tau}_n^m \right], \tag{9}$$

where

$$\tilde{\pi}_n^m = \frac{m}{\sin\theta} \tilde{P}_n^m(\cos\theta), \text{ and} \tag{10}$$

$$\tilde{\tau}_n^m = \frac{\partial}{\partial\theta} \tilde{P}_n^m(\cos\theta). \tag{11}$$

The asymmetry parameter is the integral of the cosine-weighted intensity phase function and is a measure of the amount of forward scatter from the particle:

$$g = \frac{1}{2k^2 C_{sca}} \int_0^{2\pi} \int_0^{\pi} \left(|S_1|^2 + |S_2|^2 + |S_3|^2 + |S_4|^2 \right) \cos\theta \sin\theta \; d\theta \; d\phi, \tag{12}$$

where the scattering cross section is defined as

$$C_{sca} = \frac{1}{2k^2} \int_0^{2\pi} \int_0^{\pi} \left(|S_1|^2 + |S_2|^2 + |S_3|^2 + |S_4|^2 \right) \sin\theta \; d\theta \; d\phi, \tag{13}$$

which is equivalent to

$$C_{sca} = \frac{2\pi}{k^2} \sum_{n=1}^{\infty} n(n+1) \sum_{m=-n}^{n} \left(\left| a_{nm}^{(1)} \right|^2 + \left| b_{nm}^{(1)} \right|^2 + \left| a_{nm}^{(2)} \right|^2 + \left| b_{nm}^{(2)} \right|^2 \right). \tag{14}$$

For an arbitrarily shaped particle, there may be coupling between the modes, and the scattering amplitude matrix elements S_3 and S_4 are not zero. After a fair amount of algebraic manipulations, the asymmetry parameter may be expressed as

$$\begin{aligned} g &= \frac{4\pi}{k^2 C_{sca}} \mathrm{Re} \sum_{n,m} m \left(a_{nm}^{(1)} b_{nm}^{(1)*} + a_{nm}^{(2)} b_{nm}^{(2)*} \right) \\ &\quad + in(n+2) \sqrt{\frac{(n-m+1)(n+m+1)}{(2n+1)(2n+3)}} \\ &\quad \times \left(a_{nm}^{(1)} a_{n+1m}^{(1)*} + b_{nm}^{(1)} b_{n+1m}^{(1)*} + a_{nm}^{(2)} a_{n+1m}^{(2)*} + b_{nm}^{(2)} b_{n+1m}^{(2)*} \right). \end{aligned} \quad (15)$$

Equation (15) contains a great deal of information. If, for instance, there is no correlation between the coefficients,

$$\left\langle a_{nm}^{(j)} a_{n+1m}^{(j)*} \right\rangle = \left\langle b_{nm}^{(j)} b_{n+1m}^{(j)*} \right\rangle = \left\langle a_{nm}^{(j)} b_{nm}^{(j)*} \right\rangle = 0, \quad (16)$$

then there is no preferential scattering hemisphere. This condition is necessary for a scatterer to be Lambertian.

Equation (15) also shows that there is no preferential scattering hemisphere for any individual mode $\mathbf{M}_{nm}$ or $\mathbf{N}_{nm}$. However, when more than one mode is considered, there can be preferential scattering. A preferential scattering hemisphere is the result of interference between the modes. In general, constructive interference tends to be in the forward-scatter region, leading to positive g. This phase information (and resulting scattering directionality) is contained within the incident plane wave coefficients.

For reference, we show in figure 1 the calculated asymmetry parameter as a function of radius for carbon and water spheres. For radii that are small compared to the wavelength, the asymmetry parameter is zero, since no preferential scattering hemisphere exists for isolated Rayleigh-size scatterers. As the sphere radius approaches the wavelength, the asymmetry parameter rises rapidly, corresponding to the increase in scatter in the forward direction. For the highly absorbing carbon spheres, the asymmetry parameter levels off around 0.9. As the transparent, water-sphere radius increases, the internal fields selectively intensify specific modes in the sphere through morphology-dependent resonances. Selective enhancement of specific modes tends to decrease the asymmetry parameter, since (from eq (16)) a specific mode does not have a preferential scattering hemisphere, and the normalizing scattering cross section is increased.

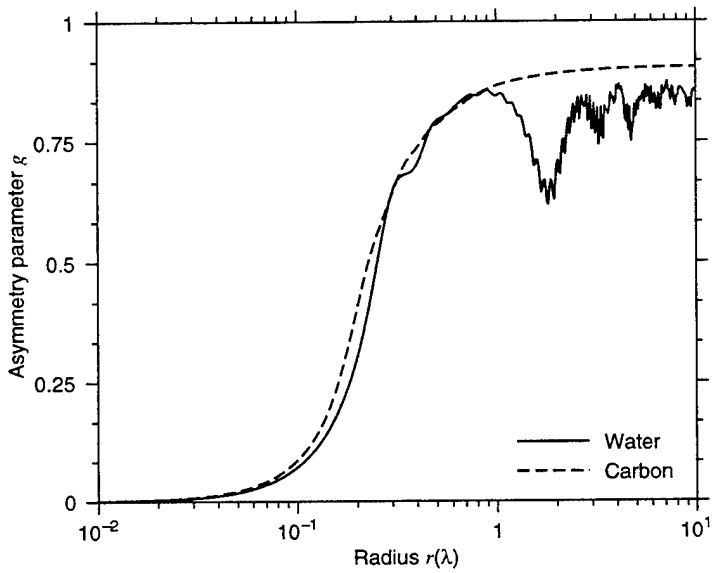

Figure 1. Asymmetry parameter of water ($n = 1.33$) and carbon ($n = 1.75+0.44i$) spheres as a function of sphere radius.

3. Aggregates

Other researchers [13–28] have recently derived solutions for the scatter from aggregate particles by considering the entire system to be composed of multiple subsystems, and by including an interaction term as part of the field incident on each subsystem. This interaction term is due to the scattered field from all other subsystems striking the subsystem of interest. The scattering coefficients for the jth subsystem, $f_{nm}^{1,j}$ and $f_{nm}^{2,j}$, can be expressed as a set of coupled linear equations,

$$f_{nm}^{1,j} = a_{nm}^{1,j} + \sum_{k \neq j} \sum_{n'} \sum_{m'} f_{n'm'}^{1,k} A_{nm}^{jkn'm'} + f_{n'm'}^{2,k} B_{nm}^{jkn'm'}, \tag{17}$$

$$f_{nm}^{2,j} = a_{nm}^{2,j} + \sum_{k \neq j} \sum_{n'} \sum_{m'} f_{n'm'}^{1,k} C_{nm}^{jkn'm'} + f_{n'm'}^{2,k} D_{nm}^{jkn'm'}, \tag{18}$$

where $a_{nm}^{n,j}$ is a function of the incident field and $A_{nm}^{jkn'm'}$, $B_{nm}^{jkn'm'}$, $C_{nm}^{jkn'm'}$, and $D_{nm}^{jkn'm'}$ are system-dependent parameters that include translation coefficients that can be used to express the vector spherical harmonics in subsystem k in terms of vector spherical harmonics in subsystem j. Once solutions for the scattering coefficients $f_{nm}^{1,j}$ and $f_{nm}^{2,j}$ are found, the total scattered field is found as the superposition of the scattered fields from all the subsystems. We can find the asymmetry parameter using equation (15) by expressing the total scattered field in terms of a single coordinate system, which is a straightforward process using the addition theorem for vector spherical harmonics and the linearity of the system.

Aggregation can affect the scatter in two ways: through interference and interaction. We can isolate the effect of interference by expressing the total scattered fields in terms of the individual scattering components. Since the total scattered electric field can be expressed as the sum of the contributions from each aggregate ($\mathbf{E}^{sca} = \sum_j \mathbf{E}_j^{sca}$), the asymmetry parameter can be expressed as

$$g = \frac{\sum\limits_{j \neq k} \int_0^{2\pi} \int_0^{\pi} \mathbf{E}_j^{sca*} \cdot \mathbf{E}_k^{sca} \cos\theta \sin\theta \; d\theta \; d\phi}{\int_0^{2\pi} \int_0^{\pi} \mathbf{E}^{sca*} \cdot \mathbf{E}^{sca} \sin\theta \; d\theta \; d\phi} + \frac{\sum\limits_{j} \int_0^{2\pi} \int_0^{\pi} \mathbf{E}_j^{sca*} \cdot \mathbf{E}_j^{sca} \cos\theta \sin\theta \; d\theta \; d\phi}{\int_0^{2\pi} \int_0^{\pi} \mathbf{E}^{sca*} \cdot \mathbf{E}^{sca} \sin\theta \; d\theta \; d\phi}. \tag{19}$$

The first term of equation (19) accounts for the interference between the fields scattered by the jth and kth subsystems. The second term of equation (19) is the sum of the individual asymmetry parameters calculated from each individual subsystem. In sections 3.1 and 3.2, we consider these terms individually. When the subsystems are far enough apart that any particle-particle interaction or interference becomes negligible, equation (19) must reduce to

$$g_o = \frac{\sum_j g_j C_{sca,j}}{C_{sca}}, \tag{20}$$

where g_j and $C_{sca,j}$ are the asymmetry parameter and scattering cross section for the isolated jth subsystem. The effects of the interaction are contained within the scattering coefficients themselves; thus, we can isolate the interaction effect by subtracting g_o from the second term of equation (19).

3.1 Interaction

Interaction between subsystems is difficult to characterize because there is mode mixing between the subsystems. One effect of the interaction is enhanced backscatter, which is due to constructive interference of rays reflecting off multiple interfaces. In the backscatter direction, the path difference of light rays striking multiple interfaces is the same when the order of the interfaces is reversed. These two rays (forward and backward traversing) interfere constructively, and the resulting intensity is enhanced. When backscattered light is enhanced, the asymmetry parameter must decrease.

Figure 2 shows the individual components of the asymmetry parameter given by equation (19) as a function of separation distance d. In this figure, the asymmetry parameter is averaged over all orientations of a scattering system composed of two $r = \lambda/2$ carbon spheres (fig. 2a) and two $r = \lambda/10$ carbon spheres (fig. 2b). The effect of enhanced backscatter is contained within the second term of equation (19) (after g_o is subtracted out). Note that the interference term is always positive, and the interaction term is always negative. For both particle systems, the interaction component is approximately proportional to d^{-2}, which is proportional to the scattered flux of one subsystem, intercepted by the other subsystem. This is to be expected, since the interaction between particles must decrease with the magnitude of the interaction field.

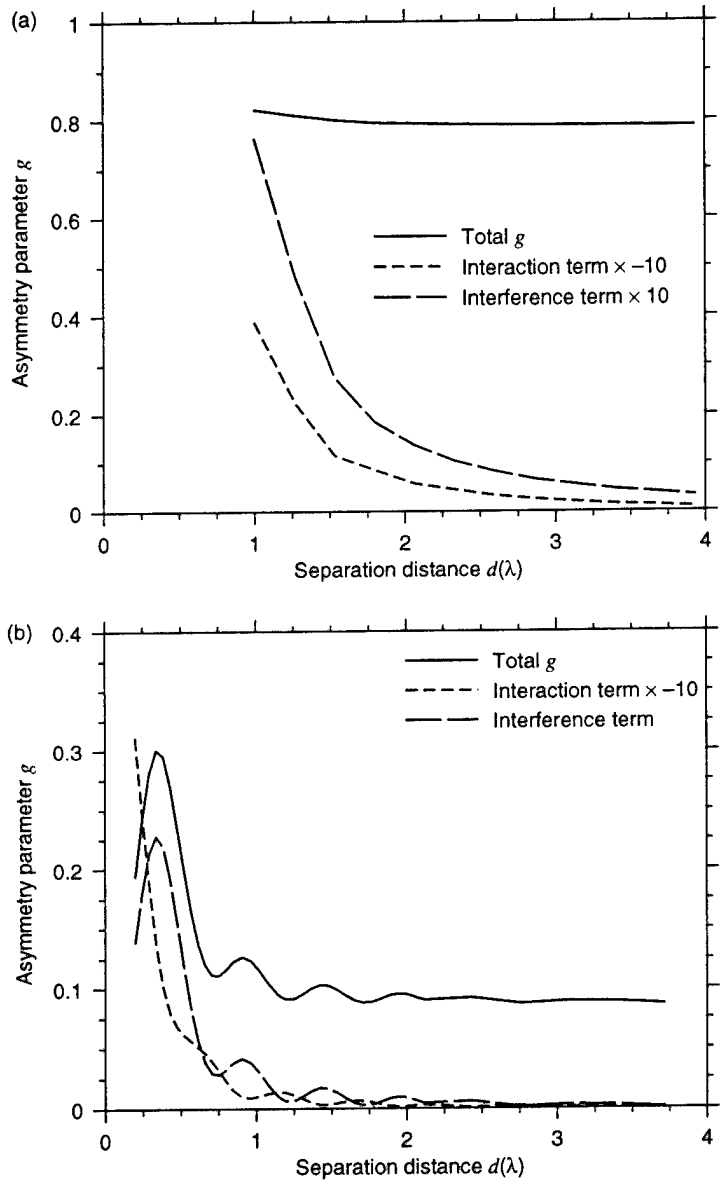

Figure 2. Asymmetry parameter as a function of separation distance d for two carbon spheres, (a) $r = \lambda/2$ and (b) $r = \lambda/10$, averaged over all orientations. Note interference term is always positive and interaction term is always negative.

3.2 Interference

Interference produces a high-frequency structure on the scattering phase function. This is illustrated in figure 3, which shows the scatter from a pair of $r = \lambda/4$ carbon spheres illuminated at broadside incidence. For comparison, the scatter from a single sphere having the same parameters is also shown. The major effect of interference is a high-frequency modulation on the scattered signals. The positions of the high-frequency maxima and minima are dependent on the positions of the aggregate subsystems. Since the scattered waves from each subsystem acquire the same phase difference in the forward direction, there is always constructive interference in this direction, and therefore, a maximum. Hence, interference tends to increase the asymmetry parameter. This is illustrated in figure 2a, which shows the individual components of the asymmetry parameter (eq (19)) as a function of separation distance d. Note that as the separation distance d increases, the interference component of the asymmetry parameter for the two-sphere aggregate is positive and asymptotically approaches 0. This is because the spatial frequency of the interference structure increases with separation distance, and a high-frequency modulation has little effect on the integration of the scattering intensities given by equation (19). In figure 2b (for $r = \lambda/10$ carbon spheres), there is much more structure in the interference component. The large maximum occurring near $d = \lambda/4$ is due to destructive interference of scattered light in the backward direction, which increases the

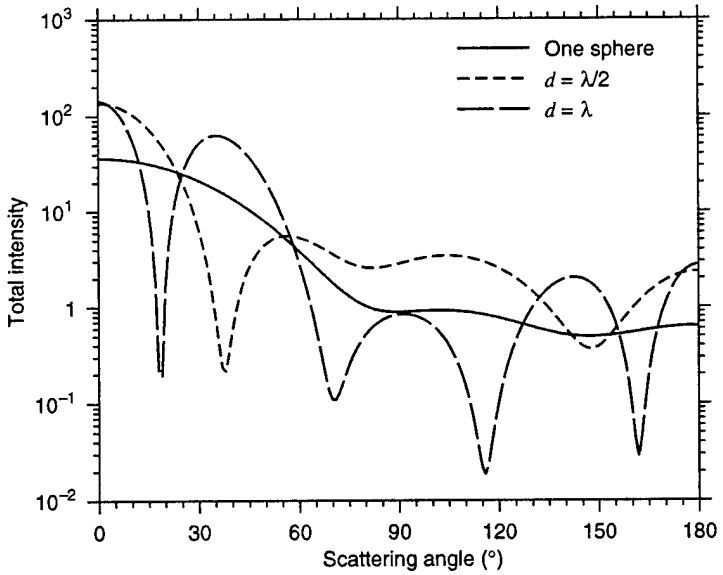

Figure 3. Intensity as a function of scattering angle for $r = \lambda/4$ carbon spheres ($n = 1.75 + 0.44i$) showing interference structure.

value of g. Subsequent maxima in the interference term occur at intervals of approximately $\lambda/2$ and are similar to the interference structure of thin films. The particulate components of a simple aggregate tend to be in contact. Figure 4a shows the asymmetry parameter as a function of radius r for two carbon spheres in contact, averaged over all orientations. The curves of this figure are significantly different from the curves of figure 2, owing to the spheres being in contact. All that remains of the interference structure is the large maximum occurring near $r = \lambda/8$ ($d = \lambda/4$), which dominates the asymmetry parameter for small sphere radii. The interference term of equation (19) remains a significant component for much larger separation distances when the spheres are in contact. The shape of the total asymmetry parameter is similar to that of the single carbon sphere (shown for comparison in fig. 1).

Figure 4b shows the percentage errors resulting in asymmetry parameter calculations when the two-sphere aggregate is assumed to be a sphere. Although equivalent-volume spheres approximate the asymmetry parameter better than equivalent-area spheres and an isolated sphere having the same radius of one of the components, the errors are still significant, especially when the aggregate components are smaller than the wavelength. As shown in figure 4a, at these small radii, the interference between the individual particles (which cannot be included in any equivalent-sphere system) plays a dominant role in the determination of the asymmetry parameter.

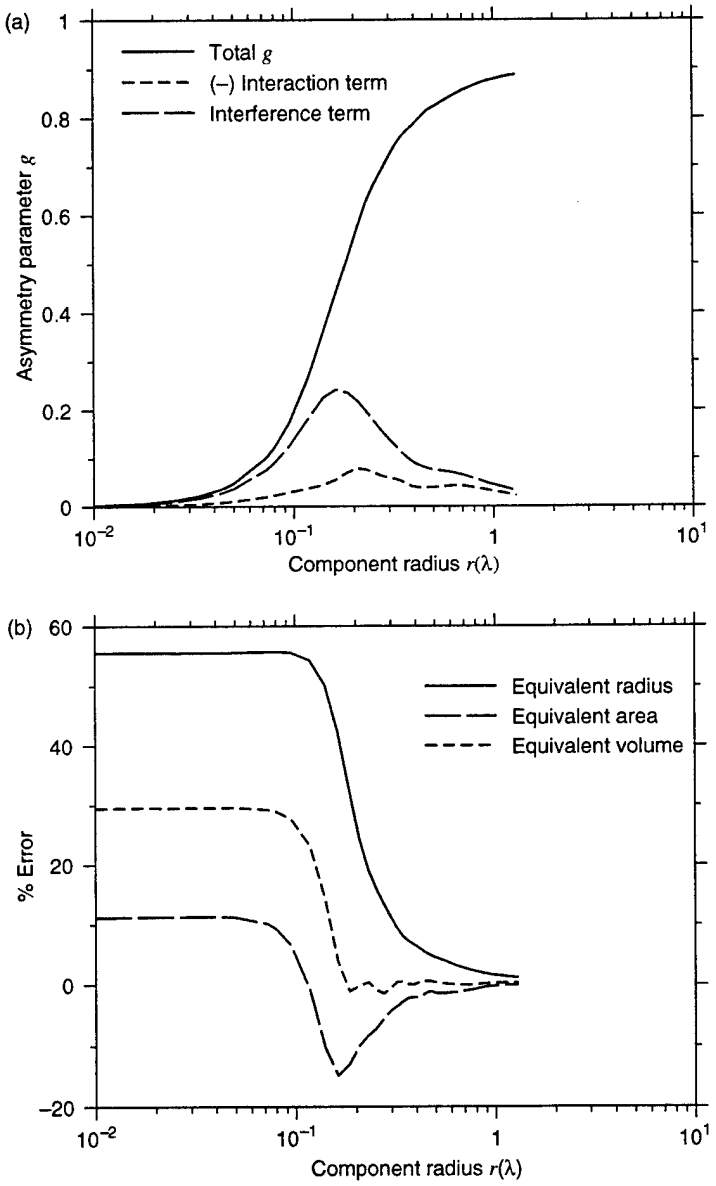

Figure 4. Asymmetry parameter: components as a function of component radius r (a) for two carbon spheres in contact, averaged over all orientations, and (b) for two-sphere aggregate compared with equivalent single carbon sphere.

4. Conclusion

In this report, we provide an expression for the asymmetry parameter of an arbitrarily shaped particle for which the scattering solution can be expressed in a multipole solution. We have considered the special case of an aggregate and have isolated the two mechanisms—interference and interaction—that affect the value of the asymmetry parameter. Interference tends to increase the asymmetry parameter by preferentially scattering light in the forward direction. Counteracting this effect is the interaction component, which accounts for enhanced backscatter.

For the two-sphere aggregates we examined, the interference effects outweigh the interaction effects. Equivalent-sphere systems do not have a mechanism to reproduce either of these effects and, consequently, provide poor approximations when these effects are significant. Although interference plays a greater role than interaction for the bisphere system, we cannot assume that it does so for other aggregate or irregular systems. As the number of surface irregularities increases (for instance, in a multifaceted ice crystal), the interaction would be expected to play a dominant role and the asymmetry parameter would be reduced. By isolating the factors that affect the asymmetry parameter, we can proceed in the parameterization of these factors as a function of the number of subparticles contained in a system and the number of surface irregularities. Such a parameterization is immediately applicable to nonspherical ice crystals in cirrus clouds.

References

1. P. Debye, "Der Lichtdruck auf Kugeln von beliebigem Material," *Ann. Phys.* **30** (1909), 57–136.

2. K.-N. Liou, *Introduction to Atmospheric Radiation*, Academic Press, San Diego (1980).

3. Y. Takano and K.-N. Liou, "Solar radiative transfer in cirrus clouds. Part I: Single-scattering and optical properties of hexagonal ice crystals," *J. Atmos. Sci.* **45** (1989), 3–19.

4. G. L. Stephens, S. C. Tsay, P. W. Stackhouse, and P. J. Flatau, "The relevance of the microphysical and radiative properties of cirrus clouds to climate and climatic feedback," *J. Atmos. Sci.* **47** (1990), 1742–1753.

5. Q. Fu, "An accurate parameterization of the solar radiative properties of cirrus clouds for climate models," *J. Climate* **9** (1996), 2058–2082.

6. K.-N. Liou, "Influence of cirrus clouds on weather and climate processes: A global perspective," *Mon. Weather Rev.* **114** (1986), 1167–1199.

7. P. N. Francis, A. Jones, R. W. Saunders, K. P. Shine, A. Slingo, and Z. Sun, "An observational and theoretical study of the radiative properties of cirrus: Some results from ICE '89," *Q. J. R. Meteorol. Soc.* **120** (1994), 809–848.

8. S. A. Ackerman and G. L. Stephens, "The absorption of solar radiation by cloud droplets: An application of anomalous diffraction theory," *J. Atmos. Sci.* **44** (1987), 1574–1588.

9. B.T.N. Evans and G. R. Fournier, "Approximations of polydispersed extinction," *Appl. Opt.* **35** (1996), 3281–3285.

10. P. Chýlek and J. D. Klett, "Extinction cross sections of nonspherical particles in the Anomalous diffraction approximation," *J. Opt. Soc. Am.* **A8** (1991), 274–281.

11. P. Chýlek and J. D. Klett, "Absorption and scattering of electromagnetic radiation by prismatic columns: Anomalous diffraction approximation," *J. Opt. Soc. Am.* **A8** (1991), 1713–1720.

12. P. Chýlek and G. Videen, "Longwave radiative properties of polydispersed hexagonal ice crystals," *J. Atmos. Sci.* **51** (1994), 175–190.

13. C. Liang and Y. T. Lo, "Scattering by two spheres," *Radio Sci.* **2** (1967), 1481–1495.

14. J. H. Bruning and Y. T. Lo, "Multiple scattering of EM waves by spheres," parts I & II, *IEEE Trans. Antennas Propag.* **AP-19** (1971), 378–400.

15. A. R. Jones, "Electromagnetic wave scattering by assemblies of particles in the Rayleigh approximation," *Proc. R. Soc. London Ser. A* **366** (1979), 111–127.

16. J. M. Gérardy and M. Ausloos, "Absorption spectrum of clusters of spheres from the general solution of Maxwell's equations: The long wavelength limit," *Phys. Rev.* **B22** (1980), 4950–4959.

17. F. Borghese, P. Denti, R. Saija, G. Toscano, and O. I. Sindoni, "Multiple electromagnetic scattering from a cluster of spheres. I: Theory," *Aerosol Sci. Technol.* **3** (1984), 227–235.

18. K. A. Fuller and G. W. Kattawar, "Consummate solution to the problem of classical electromagnetic scattering by an ensemble of spheres. I: Clusters of arbitrary configuration," *Opt. Lett.* **13** (1988), 1063–1065.

19. M. F. Iskander, H. Y. Chen, and J. E. Penner, "Optical scattering and absorption by branched chains of aerosols," *Appl. Opt.* **28** (1989), 3083–3091.

20. D. W. Mackowski, "Analysis of radiative scattering for multiple sphere configurations," *Proc. R. Soc. London Ser. A* **433** (1991), 599–614.

21. M. I. Mishchenko, "Light scattering by randomly oriented axially symmetric particles," *J. Opt. Soc. Am.* **A8** (1991), 871–882.

22. J. C. Ku and K.-H. Shim, "A comparison of solutions for light scattering and absorption by agglomerated or arbitrarily shaped particles," *J. Quant. Spectrosc. Radiat. Transfer* **47** (1992), 201–220.

23. M. I. Mishchenko and D. W. Mackowski, "Light scattering by randomly oriented bispheres," *Opt. Lett.* **19** (1994), 1604–1606.

24. D. W. Mackowski, "Calculation of total cross sections of multiple-sphere clusters," *J. Opt. Soc. Am.* **A11** (1994), 2851–2861.

25. K. A. Fuller, "Scattering and absorption cross sections of compounded spheres. I: Theory for external aggregation," *J. Opt. Soc. Am.* **A11** (1994), 3251–3260.

26. K. A. Fuller, "Scattering and absorption cross sections of compounded spheres. II: Calculations for external aggregation," *J. Opt. Soc. Am.* **A12** (1995), 881–892.

27. S. C. Hill, H. I. Saleheen, and K. A. Fuller, "Volume current method for modeling light scattering by inhomogeneously perturbed spheres," *J. Opt. Soc. Am.* **A12** (1995), 905–915.

28. G. Videen, D. Ngo, and M. B. Hart, "Light scattering from a pair of conducting, osculating spheres," *Opt. Commun.* **125** (1996), 275–287.

29. J. G. Fikioris and N. K. Uzunoglu, "Scattering from an eccentrically stratified dielectric sphere," *J. Opt. Soc. Am.* **69** (1979), 1359–1366.

30. F. Borghese, P. Denti, and R. Saija, "Optical properties of spheres containing a spherical eccentric inclusion," *J. Opt. Soc. Am.* **A9** (1992), 1327–1335.

31. F. Borghese, P. Denti, and R. Saija, "Optical properties of spheres containing several spherical inclusions," *Appl. Opt.* **33** (1994), 484–493.

32. K. A. Fuller, "Scattering and absorption cross sections of compounded spheres. III: Spheres containing arbitrarily located spherical inhomogeneities," *J. Opt. Soc. Am.* **A12** (1995), 893–904.

33. M. M. Mazumder, S. C. Hill, and P. W. Barber, "Morphology-dependent resonances in inhomogeneous spheres: Comparison of the layered T-matrix method and the time-independent perturbation method," *J. Opt. Soc. Am.* **A9** (1992), 1844–1853.

34. N. C. Skaropoulos, M. P. Ioannidow, and D. P. Chrissoulidis, "Indirect mode-matching solution to scattering from a dielectric sphere with an eccentric inclusion," *J. Opt. Soc. Am.* **A11** (1994), 1859–1866.

35. G. Videen, D. Ngo, and P. Chýlek, "Effective-medium predictions of absorption by graphitic carbon in water droplets," *Opt. Lett.* **19** (1994), 1675–1677.

36. G. Videen, D. Ngo, P. Chýlek, and R. G. Pinnick, "Light scattering from a sphere with an irregular inclusion," *J. Opt. Soc. Am.* **A12** (1995), 922–928.

Appendix. Relations for Scattering Coefficients of Two Rotated Coordinate Systems

The relations for the scattering coefficients of two rotated coordinate systems have been derived by Stein.[1] The vector spherical harmonics in the original (primed) coordinate system are related to the vector spherical harmonics in a rotated system (in which the plane wave travels in the positive z direction):

$$\mathbf{M}_{nm}^{(3)} = \sum_{m'} D_{m'}^{(n,m)} \mathbf{M}_{nm'}^{(3)'}, \tag{A-1}$$

$$\mathbf{N}_{nm}^{(3)} = \sum_{m'} D_{m'}^{(n,m)} \mathbf{N}_{nm'}^{(3)'}, \tag{A-2}$$

where the rotation coefficients $D_{m'}^{(n,m)}$ are given by

$$\begin{aligned} D_{m'}^{(n,m)} &= \exp\left[i\left(m'\alpha + m\gamma\right)\right] \left[\frac{(n+m')!\,(n-m')!}{(n+m)!\,(n-m)!}\right]^{1/2} \\ &\times \sum_{\sigma} \binom{n+m}{n-m'-\sigma} \binom{n-m}{\sigma} (-1)^{n+m-\sigma} \left[\cos\left(\beta/2\right)\right]^{2\sigma+m'+m} \\ &\times \left[\sin\left(\beta/2\right)\right]^{2n-2\sigma-m'-m} \end{aligned} \tag{A-3}$$

and α, β, and γ are Euler angles following the convention of Edmonds.[2] The coefficients in the rotated coordinate system, a_{nm} and b_{nm}, can be expressed in the unrotated coordinate system, c_{nm} and d_{nm}, as

$$a_{nm} = \sum_{m'} D_{m'}^{(n,m)} c_{nm'}, \tag{A-4}$$

$$b_{nm} = \sum_{m'} D_{m'}^{(n,m)} d_{nm'}. \tag{A-5}$$

[1] S. Stein, "Addition theorems for spherical wave functions," *Q. Appl. Math.* **19** (1961), 15–24.

[2] A. R. Edmonds, *Angular Momentum in Quantum Mechanics*, Princeton University Press, Princeton, NJ (1957).

Distribution

Admnstr
Defns Techl Info Ctr
Attn DTIC-OCP
8725 John J Kingman Rd Ste 0944
FT Belvoir VA 22060-6218

Central Intllgnc Agency Dir DB Standard
Attn GE 47 QB
Washington DC 20505

Chairman Joint Chiefs of Staff
Attn J5 R&D Div
Washington DC 20301

Defns Intllgnc Agency
Attn DT 2 Wpns & Sys Div
Washington DC 20301

Dir of Defns Rsrch & Engrg
Attn DD TWP
Attn Engrg
Washington DC 20301

Ofc of the Secy of Defns
Attn ODDRE (R&AT) G Singley
Attn ODDRE (R&AT) S Gontarek
The Pentagon
Washington DC 20301-3080

OIR CSB CRB
Attn A M Jones
RB 1413 OHM
Washington DC 20505

US Dept of Energy
Attn KK 22 K Sisson
Attn Techl Lib
Washington DC 20585

Commanding Officer
Attn NMCB23
6205 Stuart Rd Ste 101
FT Belvoir VA 22060-5275

CECOM
Attn PM GPS COL S Young
FT Monmouth NJ 07703

CECOM RDEC Electronic Systems Div Dir
Attn J Niemela
FT Monmouth NJ 07703

CECOM
Sp & Terrestrial Commctn Div
Attn AMSEL-RD-ST-MC-M H Soicher
FT Monmouth NJ 07703-5203

DARPA
Attn B Kaspar
Attn L Stotts
Attn Techl Lib
3701 N Fairfax Dr
Arlington VA 22203-1714

Dir of Chem & Nuc Ops DA DCSOPS
Attn Techl Lib
Washington DC 20301

Dpty Assist Secy for Rsrch & Techl
Attn SARD-TR R Chait
Attn SARD-TT D Chait
Attn SARD-TT F Milton Rm 3E479
Attn SARD-TT K Kominos
Attn SARD-TT R Reisman
Attn SARD-TT T Killion
Attn SARD-TT C Nash Rm 3E479
The Pentagon Rm 3E476
Washington DC 20301-0103

Hdqtrs Dept of the Army
Attn DAMO-FDQ D Schmidt
400 Army Pentagon
Washington DC 20301-0460

OSD
Attn OUSD(A&T)/ODDDR&E(R) J Lupo
The Pentagon
Washington DC 20301-7100

US Army Engrg Div
Attn HNDED FD
PO Box 1500
Huntsville AL 35807

US Army Matl Cmnd
Dpty CG for RDE Hdqtrs
Attn AMCRD BG Beauchamp
5001 Eisenhower Ave
Alexandria VA 22333-0001

US Army Matl Cmnd
Prin Dpty for Acquisition Hdqrts
Attn AMCDCG-A D Adams
5001 Eisenhower Ave
Alexandria VA 22333-0001

Distribution

US Army Matl Cmnd
Prin Dpty for Techlgy Hdqrts
Attn AMCDCG-T M Fisette
5001 Eisenhower Ave
Alexandria VA 22333-0001

US Army Mis & Spc Intllgnc Ctr
Attn AIAMS YDL
Redstone Arsenal AL 35898-5500

US Army NGIC
Attn Rsrch & Data Branch
220 7th Street NE
Charlottesville VA 22901-5396

US Army Nuc & Cheml Agency
7150 Heller Loop Ste 101
Springfield VA 22150-3198

US Army Rsrch Lab
Attn AMXRO-ICA B Mann
PO Box 12211
Research Triangle Park NC 27709-2211

US Army Strtgc Defns Cmnd
Attn CSSD H MPL Techl Lib
Attn CSSD H XM Dr Davies
PO Box 1500
Huntsville AL 35807

US Military Academy
Dept of Mathematical Sci
Attn MAJ D Engen
West Point NY 10996

USAASA
Attn MOAS-AI W Parron
9325 Gunston Rd Ste N319
FT Belvoir VA 22060-5582

Chief of Nav OPS Dept of the Navy
Attn OP 03EG
Washington DC 20350

GPS Joint Prog Ofc Dir
Attn COL J Clay
2435 Vela Way Ste 1613
Los Angeles AFB CA 90245-5500

Ofc of the Dir Rsrch and Engrg
Attn R Menz
Pentagon Rm 3E1089
Washington DC 20301-3080

Naval Surface Weapons Ctr
Attn Code B07 J Pennella
17320 Dahlgren Rd Bldg 1470 Rm 1101
Dahlgren VA 22448-5100

Special Assist to the Wing Cmndr
Attn 50SW/CCX Capt P H Bernstein
300 O'Malley Ave Ste 20
Falcon AFB CO 80912-3020

ARL Electromag Group
Attn Campus Mail Code F0250 A Tucker
University of TX
Austin TX 78712

US Army Rsrch Lab
Attn AMSRL-CI-LL Techl Lib (3 copies)
Attn AMSRL-CS-AL-TA Mail & Records Mgmt
Attn AMSRL-CS-AL-TP Techl Pub (3 copies)
Attn AMSRL-IS-EE G Videen (5 copies)
Adelphi MD 20783-1197

REPORT DOCUMENTATION PAGE

Form Approved
OMB No. 0704-0188

1. AGENCY USE ONLY *(Leave blank)*	2. REPORT DATE	3. REPORT TYPE AND DATES COVERED
	October 1997	Progress, from 1 Oct 1996 to April 1997

4. TITLE AND SUBTITLE

The Asymmetry Parameter and Aggregrate Particles

5. FUNDING NUMBERS

DA PR: B53A
PE: P61102

6. AUTHOR(S)

Gorden Videen, Ronald G. Pinnick (ARL), Dat Ngo (Ngo Co.),
Qiang Fu, and Petr Chýlek (Dalhousie University)

7. PERFORMING ORGANIZATION NAME(S) AND ADDRESS(ES)

U.S. Army Research Laboratory
Attn: AMSRL-IS-EE
2800 Powder Mill Road
Adelphi, MD 20783-1197

8. PERFORMING ORGANIZATION REPORT NUMBER

ARL-TR-1393

9. SPONSORING/MONITORING AGENCY NAME(S) AND ADDRESS(ES)

U.S. Army Research Laboratory
2800 Powder Mill Road
Adelphi, MD 20783-1197

10. SPONSORING/MONITORING AGENCY REPORT NUMBER

11. SUPPLEMENTARY NOTES

AMS code: 611102.53A11
ARL PR: 7FEJ60

12a. DISTRIBUTION/AVAILABILITY STATEMENT

Approved for public release; distribution unlimited.

12b. DISTRIBUTION CODE

13. ABSTRACT *(Maximum 200 words)*

We derive and examine the general expression for the scattering asymmetry parameter g. For aggregate particles, the asymmetry parameter is made up of two terms. One term accounts for interference effects of the electromagnetic fields radiating from the individual subsystems. The other term accounts for interaction effects of the electromagnetic fields between these subsystems. Enhanced backscatter is one phenomenon resulting from these interactions. Numerical results demonstrate that interference effects play a dominant role when the separation distance between aggregates is smaller than half the incident wavelength. As the separation distance becomes large, both interference and interaction effects drop off, and the asymmetry parameter approaches that of the individual particle constituents.

14. SUBJECT TERMS

Scatter, radiation transfer, cirrus clouds

15. NUMBER OF PAGES

28

16. PRICE CODE

17. SECURITY CLASSIFICATION OF REPORT	18. SECURITY CLASSIFICATION OF THIS PAGE	19. SECURITY CLASSIFICATION OF ABSTRACT	20. LIMITATION OF ABSTRACT
Unclassified	Unclassified	Unclassified	UL

NSN 7540-01-280-5500

Standard Form 298 (Rev. 2-89)
Prescribed by ANSI Std. Z39-18
298-102